

Supplementary Materials for
Enhanced quantum sensing with room-temperature solid-state masers

Hao Wu *et al.*

Corresponding author: Bo Zhang, bozhang_quantum@bit.edu.cn

Sci. Adv. **8**, eade1613 (2022)
DOI: 10.1126/sciadv.adel613

This PDF file includes:

Section S1 and S2
Figs. S1 and S2
Table S1
References

Section S1: Electromagnetic simulation of microwave dielectric resonators

The dielectric resonator supporting the $|X\rangle\leftrightarrow|Z\rangle$ transition among the pentacene's triplet sublevels was designed using COMSOL Multiphysics with a 2D axisymmetric model(60). The aim of the simulation is to determine the geometry of the dielectric material, i.e. strontium titanate (STO) for generating a TE_{018} electromagnetic mode resonant around 1.45 GHz (i.e. close to the pentacene's $|X\rangle\leftrightarrow|Z\rangle$ transition frequency at zero field). A TE_{018} mode of a STO resonator has been proven, so far, to be the most suitable for pentacene-doped-*p*-terphenyl masers, which simultaneously provides a relatively high magnetic filling factor (~ 0.3)(33, 35) and a high Purcell factor (3.6×10^7)(27). The overall composition of the resonator (see Fig. S1), including a STO hollow cylinder, a support made of Rexolite, a copper tuning screw, loop antennas and an oxygen-free copper cavity with a hole drilled on the wall for optical pumping, is similar to that employed in the previous studies(21, 27, 33, 35, 48). But because the dielectric constant of STO varies with suppliers, which may arise from different impurities contained in STO, the exact dimensions of the STO hollow cylinder needs to be determined by the simulation.

Prior to the simulation, we manufactured prototypes (with arbitrarily chosen dimensions) of the STO hollow cylinder, the Rexolite support and the oxygen-free copper cavity with a cooper tuning screw. After assembly of the prototype dielectric resonator, the resonance frequency of its TE_{018} mode was measured with a microwave analyzer (Keysight N9917A). We then inputted the known geometries of all prototype components in the COMSOL model and adjusted the dielectric constant of STO to fit with the experimentally determined resonance frequency. By fitting, the dielectric constant of the STO raw material used in our work was determined to be 318. It is worth noting that for simplicity of the simulation, loop antennas were not included in the model. Moreover, because the Rexolite support and the pentacene-doped *p*-terphenyl crystal shown in Fig. S1 have been verified not to change the resonance

frequency significantly, only the dielectric material (i.e. STO), the copper cavity and air were constructed in the model. The height of the copper cavity was set to be a flexible parameter since it can be adjusted by the tuning screw in experiments.

Following the determination of the dielectric constant of STO, we adjusted the geometries of the prototype STO hollow cylinder and copper cavity in the model to achieve a 1.45-GHz TE₀₁₈ mode (shown in Fig. S1) with a tunable range about 20 MHz (by adjusting the height of the copper cavity). The geometries of the crucial parts of the dielectric resonator were thus finalized.

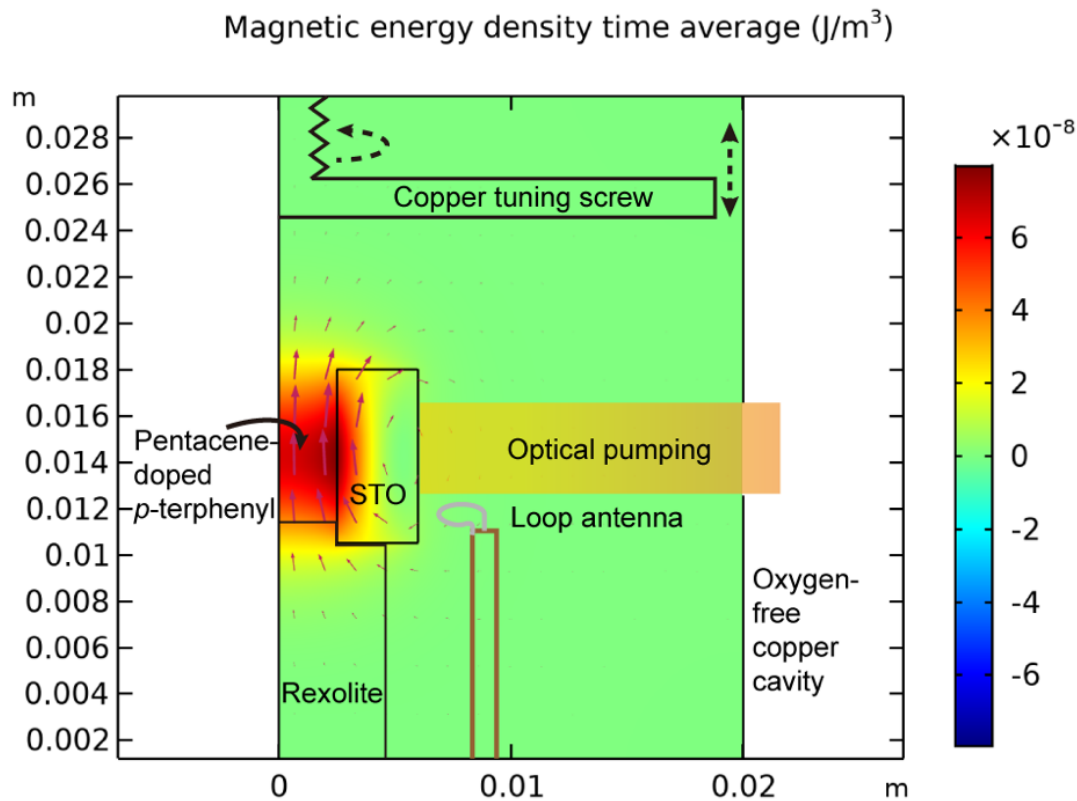


Figure. S1. A two-dimensional (2D) axisymmetric simulation of the strontium titanate (STO) microwave resonator. The heat map and red arrows represent the magnetic energy density and magnetic field vector of the TE₀₁₈ mode of the STO microwave resonator. The main components used to construct the resonator, the sample position and the optical pump path through the cavity wall are labelled.

Section S2: Configuration of a regenerative microwave oscillator

The block diagram of the regenerative microwave oscillator is shown in Fig. 2(C) of the main text. The key microwave components and equipment used are summarized in Table. S1.

Table. S1. List of the key microwave components/equipment used for the setup of the regenerative microwave oscillator

Type	Brand	Model
Isolator	TDK	11GRZO3
Amplifier	MITEQ	124758
	Qorvo	SPF5189Z
Band-pass filter	Unbranded/Generic	FBP-1420s
Power splitter	Talent Microwave	RS2DC180-S
Limiter	Mini Circuits	ZFLM-252-1WL-S+
Directional coupler	Narda	25017
	Narda-ATM	C122E-10
Variable attenuator	MERRIMAC	AUM-25A
Phase shifter	SAGE	6718-2
Logarithmic detector	ADI	AD8317
Microwave analyzer	Keysight	N9917A
Oscilloscope	Tektronix	MSO64

To measure the quality of the microwave oscillator, a transmission (S_{21}) measurement was conducted at the coupling ports of the two directional couplers shown in Fig. 2(C). To protect the microwave analyzer (Keysight N9917A) from the oscillating signals generated in the circuit, two isolators were added at the input and output ports of the analyzers. The obtained transmission spectrum is rescaled and shown in Fig. S2. The transmission linewidth was measured to be about

8 kHz which corresponds to a boosted quality factor of ~ 180000 . The similar ‘ Q -boosting’ strategy has also been used to achieve room-temperature strong coupling of a spin ensemble with microwave photons(61) and explore gain media of room-temperature solid-state masers(36).

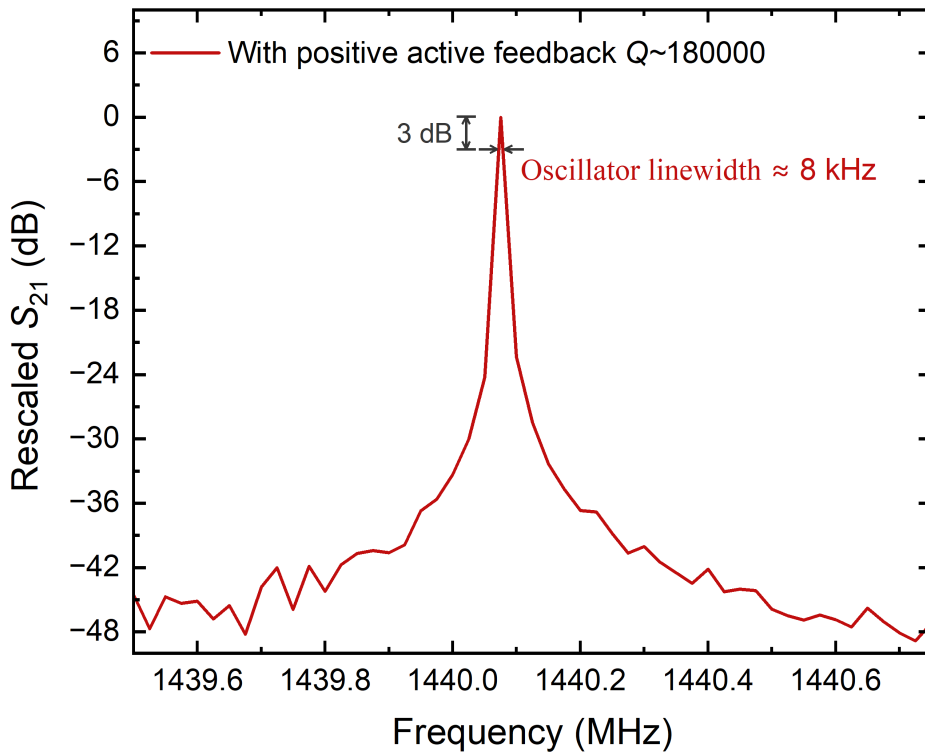


Figure. S2. Measured quality factor (Q) of the regenerative microwave oscillator. The linewidth was determined by the frequency difference of the two -3-dB points straddling the central frequency. The quality factor is the ratio of the central frequency to the linewidth.

REFERENCES AND NOTES

1. C. L. Degen, F. Reinhard, P. Cappellaro, Quantum sensing. *Rev. Mod. Phys.* **89**, 035002 (2017).
2. G. Wolfowicz, F. J. Heremans, C. P. Anderson, S. Kanai, H. Seo, A. Gali, G. Galli, D. D. Awschalom, Quantum guidelines for solid-state spin defects. *Nat. Rev. Mater.* **6**, 906–925 (2021).
3. J. F. Barry, J. M. Schloss, E. Bauch, M. J. Turner, C. A. Hart, L. M. Pham, R. L. Walsworth, Sensitivity optimization for NV-diamond magnetometry. *Rev. Mod. Phys.* **92**, 015004 (2020).
4. H. Clevenson, M. E. Trusheim, C. Teale, T. Schröder, D. Braje, D. Englund, Broadband magnetometry and temperature sensing with a light-trapping diamond waveguide. *Nat. Phys.* **11**, 393–397 (2015).
5. K. Jensen, N. Leefer, A. Jarmola, Y. Dumeige, V. M. Acosta, P. Kehayias, B. Patton, D. Budker, Cavity-enhanced room-temperature magnetometry using absorption by nitrogen-vacancy centers in diamond. *Phys. Rev. Lett.* **112**, 160802 (2014).
6. F. Dolde, H. Fedder, M. W. Doherty, T. Nöbauer, F. Rempp, G. Balasubramanian, T. Wolf, F. Reinhard, L. C. L. Hollenberg, F. Jelezko, J. Wrachtrup, Electric-field sensing using single diamond spins. *Nat. Phys.* **7**, 459–463 (2011).
7. R. Li, F. Kong, P. Zhao, Z. Cheng, Z. Qin, M. Wang, Q. Zhang, P. Wang, Y. Wang, F. Shi, J. Du, Nanoscale electrometry based on a magnetic-field-resistant spin sensor. *Phys. Rev. Lett.* **124**, 247701 (2020).
8. G. Kucsko, P. C. Maurer, N. Y. Yao, M. Kubo, H. J. Noh, P. K. Lo, H. Park, M. D. Lukin, Nanometre-scale thermometry in a living cell. *Nature* **500**, 54–58 (2013).
9. C.-F. Liu, W.-H. Leong, K. Xia, X. Feng, A. Finkler, A. Denisenko, J. Wrachtrup, Q. Li, R.-B. Liu, Ultra-sensitive hybrid diamond nanothermometer. *Natl. Sci. Rev.* **8**, nwaa194 (2021).
10. G.-Q. Liu, X. Feng, N. Wang, Q. Li, R.-B. Liu, Coherent quantum control of nitrogen-

- vacancy center spins near 1000 Kelvin. *Nat. Commun.* **10**, 1344 (2019).
11. F. Shi, F. Kong, P. Zhao, X. Zhang, M. Chen, S. Chen, Q. Zhang, M. Wang, X. Ye, Z. Wang, Z. Qin, X. Rong, J. Su, P. Wang, P. Z. Qin, J. Du, Single-DNA electron spin resonance spectroscopy in aqueous solutions. *Nat. Methods* **15**, 697–699 (2018).
 12. J. M. Taylor, P. Cappellaro, L. Childress, L. Jiang, D. Budker, P. R. Hemmer, A. Yacoby, R. Walsworth, M. D. Lukin, High-sensitivity diamond magnetometer with nanoscale resolution. *Nat. Phys.* **4**, 810–816 (2008).
 13. W. M. Itano, J. C. Bergquist, J. J. Bollinger, J. Gilligan, D. Heinzen, F. Moore, M. Raizen, D. J. Wineland, Quantum projection noise: Population fluctuations in two-level systems. *Phys. Rev. A* **47**, 3554–3570 (1993).
 14. A. Dréau, M. Lesik, L. Rondin, P. Spinicelli, O. Arcizet, J. F. Roch, V. Jacques, Avoiding power broadening in optically detected magnetic resonance of single NV defects for enhanced dc magnetic field sensitivity. *Phys. Rev. B* **84**, 195204 (2011).
 15. L. C. Rondin, J.-P. Tetienne, T. Hingant, J.-F. Roch, P. Maletinsky, V. Jacques, Magnetometry with nitrogen-vacancy defects in diamond. *Rep. Prog. Phys.* **77**, 056503 (2014).
 16. M. Oxborrow, J. D. Breeze, N. M. Alford, Room-temperature solid-state maser. *Nature* **488**, 353–356 (2012).
 17. J. D. Breeze, E. Salvadori, J. Sathian, N. M. Alford, C. W. M. Kay, Continuous-wave room-temperature diamond maser. *Nature* **555**, 493–496 (2018).
 18. L. Jin, M. Pfender, N. Aslam, P. Neumann, S. Yang, J. Wrachtrup, R.-B. Liu, Proposal for a room-temperature diamond maser. *Nat. Commun.* **6**, 8251 (2015).
 19. M. Jiang, H. Su, Z. Wu, X. Peng, D. Budker, Floquet maser. *Sci. Adv.* **7**, eabe0719 (2021).
 20. D. M. Arroo, N. M. Alford, J. D. Breeze, Perspective on room-temperature solid-state

- masers. *Appl. Phys. Lett.* **119**, 140502 (2021).
21. E. Salvadori, J. D. Breeze, K.-J. Tan, J. Sathian, B. Richards, M. W. Fung, G. Wolfowicz, M. Oxborrow, N. M. Alford, C. W. M. Kay, Nanosecond time-resolved characterization of a pentacene-based room-temperature MASER. *Sci. Rep.* **7**, 41836 (2017).
22. J. Wrachtrup, C. Von Borczyskowski, J. Bernard, M. Orrit, R. Brown, Optical detection of magnetic resonance in a single molecule. *Nature* **363**, 244–245 (1993).
23. H. Zheng, J. Xu, G. Z. Iwata, T. Lenz, J. Michl, B. Yavkin, K. Nakamura, H. Sumiya, T. Ohshima, J. Isoya, J. Wrachtrup, A. Wickenbrock, D. Budker, Zero-field magnetometry based on nitrogen-vacancy ensembles in diamond. *Phys. Rev. Applied* **11**, 064068 (2019).
24. A. K. Vershovskii, A. K. Dmitriev, A weak magnetic field sensor based on nitrogen-vacancy color centers in a diamond crystal. *Tech. Phys.* **65**, 1301–1306 (2020).
25. A. Angerer, K. Streltsov, T. Astner, S. Putz, H. Sumiya, S. Onoda, J. Isoya, W. J. Munro, K. Nemoto, J. Schmiedmayer, J. Majer, Superradiant emission from colour centres in diamond. *Nat. Phys.* **14**, 1168–1172 (2018).
26. A. J. Lotka, Undamped oscillations derived from the law of mass action. *J. Am. Chem. Soc.* **42**, 1595–1599 (1920).
27. J. Breeze, K.-J. Tan, B. Richards, J. Sathian, M. Oxborrow, N. M. Alford, Enhanced magnetic Purcell effect in room-temperature masers. *Nat. Commun.* **6**, 6215 (2015).
28. J. Köhler, Magnetic resonance of a single molecular spin. *Phys. Rep.* **310**, 261–339 (1999).
29. J. Köhler, J. A. J. M. Disselhorst, M. C. J. M. Donckers, E. J. J. Groenen, J. Schmidt, W. E. Moerner, Magnetic resonance of a single molecular spin. *Nature* **363**, 242–244 (1993).
30. J. Wrachtrup, C. Von Borczyskowski, Variation of triplet state parameters of single pentacene molecules in a *p*-terphenyl single crystal. *J. Lumin.* **64**, 13–18 (1995).
31. T.-C. Yang, D. J. Sloop, S. I. Weissman, T.-S. Lin, Zero-field magnetic resonance of the

- photo-excited triplet state of pentacene at room temperature. *J. Chem. Phys.* **113**, 11194–11201 (2000).
32. J. Lang, D. J. Sloop, T.-S. Lin, Dynamics of *p*-terphenyl crystals at the phase transition temperature: A zero-field epr study of the photoexcited triplet state of pentacene in *p*-terphenyl crystals. *J. Phys. Chem. A* **111**, 4731–4736 (2007).
33. H. Wu, S. Mirkhanov, W. Ng, M. Oxborrow, Bench-top cooling of a microwave mode using an optically pumped spin refrigerator. *Phys. Rev. Lett.* **127**, 053604 (2021).
34. D. Ham, A. Hajimiri, Virtual damping and Einstein relation in oscillators. *IEEE J. Solid-State Circuits* **38**, 407–418 (2003).
35. J. D. Breeze, E. Salvadori, J. Sathian, N. M. Alford, C. W. M. Kay, Room-temperature cavity quantum electrodynamics with strongly coupled Dicke states. *npj Quantum Inf.* **3**, 40 (2017).
36. W. Ng, S. Zhang, H. Wu, I. Nevjestic, A. J. White, M. Oxborrow, Exploring the triplet spin dynamics of the charge-transfer co-crystal phenazine/1, 2, 4, 5-tetracyanobenzene for potential use in organic maser gain media. *J. Phys. Chem. C* **125**, 14718–14728 (2021).
37. E. M. Purcell, H. C. Torrey, R. V. Pound, Resonance absorption by nuclear magnetic moments in a solid. *Phys. Rev.* **69**, 37–38 (1946).
38. B. J. Shields, Q. P. Unterreithmeier, N. P. de Leon, H. Park, M. D. Lukin, Efficient readout of a single spin state in diamond via spin-to-charge conversion. *Phys. Rev. Lett.* **114**, 136402 (2015).
39. D. Le Sage, L. M. Pham, N. Bar-Gill, C. Belthangady, M. D. Lukin, A. Yacoby, R. L. Walsworth, Efficient photon detection from color centers in a diamond optical waveguide. *Phys. Rev. B* **85**, 121202 (2012).
40. J. M. Schloss, J. F. Barry, M. J. Turner, R. L. Walsworth, Simultaneous broadband vector magnetometry using solid-state spins. *Phys. Rev. Appl.* **10**, 034044 (2018).

41. T. Wolf, P. Neumann, K. Nakamura, H. Sumiya, T. Ohshima, J. Isoya, J. Wrachtrup, Subpicotesla diamond magnetometry. *Phys. Rev. X* **5**, 041001 (2015).
42. G. Chatzidrosos, A. Wickenbrock, L. Bougas, N. Leefer, T. Wu, K. Jensen, Y. Dumeige, D. Budker, Miniature cavity-enhanced diamond magnetometer. *Phys. Rev. Applied* **8**, 044019 (2017).
43. T. Xie, F. Shi, S. Chen, M. Guo, Y. Chen, Y. Zhang, Y. Yang, X. Gao, X. Kong, P. Wang, K. Tateishi, T. Uesaka, Y. Wang, B. Zhang, J. Du, Mesoscopic magnetic resonance spectroscopy with a remote spin sensor. *Phys. Rev. Appl.* **9**, 064003 (2018).
44. J. Jeske, J. H. Cole, A. D. Greentree, Laser threshold magnetometry. *New J. Phys.* **18**, 013015 (2016).
45. H. Clevenson, L. M. Pham, C. Teale, K. Johnson, D. Englund, D. Braje, Robust high-dynamic-range vector magnetometry with nitrogen-vacancy centers in diamond. *Appl. Phys. Lett.* **112**, 252406 (2018).
46. Y. Dumeige, J.-F. Roch, F. Bretenaker, T. Debuisschert, V. Acosta, C. Becher, G. Chatzidrosos, A. Wickenbrock, L. Bougas, A. Wilzewski, D. Budker, Infrared laser threshold magnetometry with a NV doped diamond intracavity etalon. *Opt. Express* **27**, 1706–1717 (2019).
47. S. Raman Nair, L. J. Rogers, D. J. Spence, R. P. Mildren, F. Jelezko, A. D. Greentree, T. Volz, J. Jeske, Absorptive laser threshold magnetometry: Combining visible diamond Raman lasers and nitrogen-vacancy centres. *Mat. Quantum Technol.* **1**, 025003 (2021).
48. H. Wu, X. Xie, W. Ng, S. Mehanna, Y. Li, M. Attwood, M. Oxborrow, Room-temperature quasi-continuous-wave pentacene maser pumped by an invasive Ce:YAG luminescent concentrator. *Phys. Rev. Appl.* **14**, 064017 (2020).
49. D. A. Hopper, "Preparing and Measuring Single Spins in Diamond at Room Temperature", thesis, University of Pennsylvania (2019).

50. E. R. Eisenach, J. F. Barry, M. F. O'Keeffe, J. M. Schloss, M. H. Steinecker, D. R. Englund, D. A. Braje, Cavity-enhanced microwave readout of a solid-state spin sensor. *Nat. Commun.* **12**, 1357 (2021).
51. J. Ebel, T. Joas, M. Schalk, P. Weinbrenner, A. Angerer, J. Majer, F. Reinhard, Dispersive readout of room-temperature spin qubits. *Quantum Sci. Technol.* **6**, 03LT01 (2021).
52. H. Kraus, V. A. Soltamov, D. Riedel, S. Väth, F. Fuchs, A. Sperlich, P. G. Baranov, V. Dyakonov, G. V. Astakhov, Room-temperature quantum microwave emitters based on spin defects in silicon carbide. *Nat. Phys.* **10**, 157–162 (2014).
53. M. Jiang, H. Su, A. Garcon, X. Peng, D. Budker, Search for axion-like dark matter with spin-based amplifiers. *Nat. Phys.* **17**, 1402–1407 (2021).
54. A. Hahl Felix, L. Lindner, X. Vidal, T. Luo, T. Ohshima, S. Onoda, S. Ishii, M. Zaitsev Alexander, M. Capelli, C. Gibson Brant, D. Greentree Andrew, J. Jeske, Magnetic-field-dependent stimulated emission from nitrogen-vacancy centers in diamond. *Sci. Adv.* **8**, eabn7192 (2022).
55. H. Wu, W. Ng, S. Mirkhanov, A. Amirzhan, S. Nitnara, M. Oxborrow, Unraveling the room-temperature spin dynamics of photoexcited pentacene in its lowest triplet state at zero field. *J. Phys. Chem. C* **123**, 24275–24279 (2019).
56. P. W. Bridgman, "Certain physical properties of single crystals of tungsten, antimony, bismuth, tellurium, cadmium, zinc, and tin" in *Collected Experimental Papers, Volume III* (Harvard University Press, 2013), pp. 1851–1932.
57. C. P. Keijzers, E. J. Reijerse, J. Schmidt, *Pulsed EPR: A new field of applications* (North Holland, 1989).
58. N. M. Atherton, *Principles of electron spin resonance* (Ellis Horwood Limited, 1993).
59. K. Takeda, "Studies on dynamic nuclear polarization using photo-excited triplet electron spins," thesis, Kyoto University (2003).

60. M. Oxborrow, Traceable 2-D finite-element simulation of the whispering-gallery modes of axisymmetric electromagnetic resonators. *IEEE Trans. Microw. Theory Techn.* **55**, 1209–1218 (2007).
61. G. Boero, G. Gualco, R. Lisowski, J. Anders, D. Suter, J. Brugger, Room temperature strong coupling between a microwave oscillator and an ensemble of electron spins. *J. Magn. Reson.* **231**, 133–140 (2013).